Oral Lactoferrin Results in T Cell – Dependent Tumor Inhibition of Head and Neck Squamous Cell Carcinoma *In vivo*

Jeffrey S. Wolf,[1,3] Guoyan Li,[1] Atul Varadhachary,[3] Karel Petrak,[3] Mark Schneyer,[1] Daqing Li,[4] Julina Ongkasuwan,[1] Xiaoyu Zhang,[1] Rodney J. Taylor,[1] Scott E. Strome,[1,2] and Bert W. O'Malley, Jr.[4]

Abstract

Purpose: Human lactoferrin is a naturally occurring glycoprotein that inhibits cancer growth. Our purpose was to evaluate recombinant human lactoferrin as a chemotherapeutic agent against head and neck squamous cell carcinoma.

Experimental Design: Controlled experiments both *in vitro* and in the murine model evaluating both the effect and mechanism of lactoferrin on cancer growth.

Results: In both human and murine cell lines, lactoferrin induced dose-dependent growth inhibition. Using flow cytometric analysis, lactoferrin was shown to induce G_1-G_0 growth arrest. This arrest seemed to be modulated by down-regulation of cyclin D1. In the *in vitro* model, luminex data revealed that lactoferrin inhibited cellular release of proinflammatory and prometastatic cytokines, including interleukin-8, interleukin-6, granulocyte macrophage colony-stimulating factor, and tumor necrosis factor-α. Lactoferrin up-regulated the cellular activation of nuclear factor-κB within 4 h of cellular exposure. In C3h/HeJ mice implanted with SCCVII tumors, orally delivered lactoferrin inhibited tumor growth by 75% compared with control mice. Immunohistochemical analysis of harvested tumors revealed up to 20-fold increases of lymphocytes within treated animals. When mice were depleted of $CD3^+$ cells, all lactoferrin-induced tumor inhibition was abrogated.

Conclusion: We conclude that human recombinant lactoferrin can inhibit the growth of head and neck squamous cell carcinoma via direct cellular inhibition as well as systemically via immunomodulation. Our data support the study of human lactoferrin as an immunomodulatory compound with therapeutic potential.

Lactoferrin is an 80-kDa member of the transferrin family of iron-binding glycoproteins (1, 2). The protein is naturally occurring and is present in mammalian exocrine secretions, including breast milk, tears, nasal and bronchial mucus, cervical mucus, and seminal fluid (3, 4). Lactoferrin has multiple known biological activities, including iron regulation, cellular growth and differentiation, antimicrobial defense, anti-inflammatory activity, and cancer protection (3, 5, 6). Many of the functions of lactoferrin are related to immune activation and modulation (7). It is hypothesized that immunomodulation by lactoferrin contributes to the lower rate of respiratory infections and malignancies in breast-fed infants, but the exact mechanism of action of lactoferrin on the immune system is not currently understood (8 – 10). Specifically, the relative effect of lactoferrin on intrinsic cellular proliferation and immunomodulatory response is unknown.

Direct inhibition of cellular growth is one mechanism by which lactoferrin may inhibit cancer growth. Recent data have shown that lactoferrin induces direct cell cycle arrest in both breast and head and neck cancer cell lines (11, 12). Additionally, lactoferrin can decrease cellular release of the proinflammatory cytokines, including interleukin-1 (IL-1), IL-6, IL-4, and tumor necrosis factor-α, recognized for their importance in maintaining cellular viability and a malignant phenotype (13 – 17). Finally, lactoferrin decreases the activity of the transcription factor nuclear factor-κB (NF-κB; ref. 13). NF-κB is constitutively activated in head and neck squamous cell carcinoma (HNSCCA), and inhibition of this activation decreases cellular viability. Despite such well-defined mechanisms for direct lactoferrin inhibition of tumor growth *in vitro*, the specific mechanism of growth inhibition *in vivo* is not understood.

Aside from the direct tumor cell growth inhibition, cellular immunity may also be enhanced by lactoferrin. For example,

Authors' Affiliations: [1]Department of Otorhinolaryngology-Head and Neck Surgery and [2]Program in Oncology, Stewart and Marlene Greenebaum Cancer Center, University of Maryland School of Medicine, Baltimore, Maryland; [3]Agennix, Inc., Houston, Texas; and [4]Department of Otorhinolaryngology-Head and Neck Surgery, University of Pennsylvania School of Medicine, Philadelphia, Pennsylvania

Received 8/10/06; revised 10/22/06; accepted 12/7/06.

Grant support: NIH grant 5R03DE015428 (J.S. Wolf) and American Academy of Otolaryngology-Head and Neck Surgery/American Head and Neck Society Young Investigators Award (J.S. Wolf).

The costs of publication of this article were defrayed in part by the payment of page charges. This article must therefore be hereby marked *advertisement* in accordance with 18 U.S.C. Section 1734 solely to indicate this fact.

Note: S.E. Strome and B.W. O'Malley, Jr. are co-senior authors.

Disclosure: B.W. O'Malley, Jr. is a member of the Scientific Advisory Board and hold equity options in Agennix, Inc.

Requests for reprints: Jeffrey S. Wolf, Department of Otorhinolaryngology-Head and Neck Surgery, University of Maryland School of Medicine, Suite 500, 16 South Eutaw Street, Baltimore, MD 21201. Phone: 410-328-1887; Fax: 410-328-5827; E-mail: jwolf@smail.umaryland.edu.

doi:10.1158/1078-0432.CCR-06-2008

lactoferrin contributes to an increased Th1 response, which may explain the lower rate of allergies in breast-fed children (18). Similarly, oral lactoferrin induces IL-18 release from murine intestinal epithelium, where it increases $CD4^+$, $CD8^+$, and natural killer activity (19, 20). Finally, oral lactoferrin has recently been shown to reconstitute the circulating and splenic $CD4^+$ and $CD8^+$ cell population in mice treated with cyclophosphamide (21). Most significantly, this increase in lymphocytes proved functional via reconstitution of the type IV hypersensitivity reaction in these mice (21).

Recent studies have suggested that lactoferrin holds promise as a cancer therapeutic agent. Lactoferrin treatment reduces colonic carcinogenesis in rats and decreases solid tumor growth and metastases in mice (22–24) We have previously published data on the effect of lactoferrin on HNSCCA showing tumor inhibition by i.v., oral, and i.t. dosing (25, 26). We have shown that in the murine model, lactoferrin-induced growth inhibition of floor of mouth tumors is equal to that of the most common chemotherapeutic agent used for the treatment of HNSCCA (i.e., cisplatinum). The mechanism of this tumor inhibition remains to be discerned, but oral lactoferrin dosing was associated with increases in gut release of IL-18, natural killer activation, and quantity of serum $CD8^+$ cells (26).

The lactoferrin receptor is expressed in many mammalian tissues, including intestine, heart, spleen, liver, monocytes, lymphocytes, platelets, and salivary glands (27–30). The lactoferrin receptors found in the intestinal epithelium overlying peyers patches have the highest specific binding capability when compared with lactoferrin receptors at other sites (30). The murine lactoferrin receptor has 87% homology with the human receptor and shows binding specific for human, mouse, and bovine lactoferrin (28, 31, 32). Recent data have shown the presence of the lactoferrin receptor on carcinoma cell lines (29).

Despite the data showing that lactoferrin inhibits the growth of SCC of the head and neck, the mechanism of growth inhibition remains uncertain. Elucidating the mechanism of action of lactoferrin will allow us to evaluate its potential as a chemotherapeutic agent and to plan future studies to determine its role in clinical medicine. In this study, we aimed to identify the key mechanism(s) of lactoferrin-induced tumor growth inhibition. We focused our attention on the effect of lactoferrin on HNSCCA *in vitro* and *in vivo*. Our data show iron-independent, lactoferrin-induced, dose-dependent cellular inhibition of SCC cell lines that is associated with decreases in cyclin D1 and increases in P19. We found that lactoferrin also reduces the cellular production of key proinflammatory and prometastatic cytokines. To further study the mechanism of lactoferrin growth inhibition, we used orthotopic and flank tumor models to show that lactoferrin inhibits HNSCCA *in vivo* and to show that this inhibition is associated with marked increases of lymphocytic infiltration into tumors. By depleting mice of lymphocytes, all tumor inhibition was abrogated, suggesting that lactoferrin-induced tumor inhibition is the result of immunomodulation. These important findings as well as its known safety profile point to lactoferrin as a possible chemotherapeutic agent in the treatment of head and neck cancer.

Materials and Methods

Cell lines. SCCVII cell line is a spontaneously arising murine SCC (33). O12 cell lines are well characterized and derived from human SCC of the head and neck. UMSCC-9, UMSCC-38, and UMSCC-11B lines were derived from human SCC of the upper aerodigestive tract, with informed consent, at the University of Michigan (Ann Arbor, MI) and obtained from Dr. Thomas Carey. The cell lines were cultured in Eagle's MEM supplemented with 10% fetal bovine serum and penicillin/streptomycin and maintained in 5% CO_2 incubators at 37°C.

Animals. C3H/HeJ mice and BALB/c were purchased from Charles River laboratories (Wilmington, MA). The animal protocols were approved by the University of Maryland's Institutional Animal Care and Use Committee. The animal care facilities at the University of Maryland meet requirements of federal law (89-544 and 91-579) and NIH regulations and are accredited by the American Association for Assessment and Accreditation of Laboratory Animal Care International. C3h/Hej or BALB/c mice, 6 to 10 weeks old, were anesthetized using i.p. ketamine and xylazine, and a 0.1-mL suspension of 5×10^5 SCCVII cells in Hanks Buffered Saline Solution was injected s.c. in the floor of the mouth or flank.

Tumors were allowed to grow for a period of 5 days. On day 5, mice with orthotopic tumors were anesthetized with i.p. avertin to adequate depth of anesthesia as determined by toe pinch. After betadine skin cleaning, a submental skin incision was done with sharp scissors. A dissection into the floor of the mouth musculature with fine scissors revealed the tumors. Tumors were measured in three dimensions with calipers. The wounds were closed with vicryl sutures. After 10 days of oral lactoferrin dosing, mice were anesthetized, and tumors were exposed, measured, and harvested. After serum was collected, mice were then sacrificed.

For flank tumors, mice tumor volumes were measured daily using the formula: (width^2 × length) / 2. Statistical analysis was done using Student's *t* test.

Using a 20-gauge ball-tip feeding needle, human recombinant lactoferrin (Agennix, Houston, TX) was delivered enterally from days 5 to 15 in varying doses. The lactoferrin was delivered into the stomach of the mice. No anesthesia was used for oral gavage feeding.

Measurement of cell proliferation by 3-(4,5-dimethylthiazol-2-yl)-2,5-diphenyltetrazolium bromide assay. Murine cell line SCCVII and human cell lines O12 were plated in a 96-well microtiter plate and incubated overnight. Cells were washed twice with PBS and exposed to varying doses of human recombinant lactoferrin (Agennix) ranging from 0 to 250 μmol/L in serum-free KGM. Cell density was determined using an 3-(4,5-dimethylthiazol-2-yl)-2,5-diphenyltetrazolium bromide (MTT) cell proliferation assay (Boehringer Mannheim, Indianapolis, IN) per manufacturer's instructions. MTT-labeling reagent was added at daily from days 1 to 6 after lactoferrin treatment, and colorimetric absorbance values were measured at 570 nm by a microplate reader (Bio-Tek Systems, Winooski, VT). For iron saturation experiments, lactoferrin was saturated with elemental iron at a 2:1 molar ratio (iron/lactoferrin) for 10 min before adding it to the medium. Cell density was again determined using an MTT cell proliferation assay (Boehringer Mannheim). MTT-labeling reagent was added at daily from days 1 to 6 after lactoferrin treatment, and colorimetric absorbance values were measured at 570 nm by a microplate reader (Bio-Tek Systems). Statistical analysis was done using Student's *t* test.

Measurement of NF-κB activity. The determination of the NF-κB DNA binding activity was done using both electrophoretic mobility shift assay and NF-κB–specific ELISA.

UMSCC9 and SCCVII cells were cultured with lactoferrin (250 μmol/L), and nuclear extracts were harvested at 30 and 60 min using the method of Beg with minor modifications (34). Briefly, cells were rinsed with PBS and harvested from tissue culture flasks by gentle scraping. After spinning down the cells and removing the PBS, an equivalent volume of lysis buffer was added to resuspend the cell pellet. A protease inhibitor cocktail tablet (Complete Mini, Boehringer, Mannheim, Germany) was added per 10 mL of lysis buffer before use. Then samples were spun at 18,000 × *g* for 20 min at 4°C. Supernatants were aliquoted, snap-frozen, and stored at −80°C.

The protein concentration was determined by the method of Lowry using bovine serum albumin as a standard. Electrophoretic mobility shift assay was done using electrophoretic mobility shift assay chemiluminescence kit (Pierce, Rockford, IL) according to the manufacturer's protocols. A biotin-labeled oligonucleotide containing an NF-κB DNA-binding consensus sequence 5′-AGTTGAGGG-GACTTTCCCAGGC-3′ (Panomics, Inc., Fremont, CA) and an unlabeled oligonucleotide 5′-AGTTGAGGCGACTTTCCCAGGC-3′ were used to study NF-κB DNA binding activity. Oct-1 was used as control oligonucleotide. Briefly, nuclear extracts were preincubated in a reaction mixture for 20 min, and biotin end-labeled oligonucleotide containing the NF-κB consensus sequence was added. Five microliters of loading buffer was added to each sample. A 20-μL aliquot of the samples was electrophoresed through a 6% nondenaturing polyacrylamide gel. Finally, the gel was dried and exposed to X-ray film.

NF-κB DNA binding activity was assessed with transactive motif NF-κB transcription factor assay kits (Active Motif, Rixensart, Belgium) according to the manufacturer's instructions. This ELISA-like test measures the level of the active form of NF-κB contained in cell extracts specifically able to bind to an oligonucleotide containing the NF-κB consensus site (5′-GGGACTTTCC-3′) attached to a 96-well plate (35). UMSCC9, SCCVII, and UMSCC11B cell lines were incubated with lactoferrin (250 μmol/L) and/or 500 pg/mL IL-1α (positive control). Nuclear extracts were harvested at specific time points; 20-μg extracts were added to the 96-well plates. The binding of NF-κB to the DNA was visualized by anti–p65/Rel-A antibodies that specifically recognize activated NF-κB. Antibody binding was determined as absorbance values at 450 nm.

Flow cytometric analysis. For cell cycle analysis, 1×10^5 SCCVII or O12 cells were incubated in 25-cm^2 flasks. Human recombinant lactoferrin (250 μmol/L) was added to the medium at 24 h, and the cells were incubated for up to 48 h. Adherent cells were trypsinized and fixed in 70% ethanol at 4°C.

Before analysis, cells were washed once in PBS and resuspended in 1 mL propidium iodide working solution (PBS, 0.5 mg/mL RNase, and 0.1 mg/mL propidium iodide). Cell cycle distribution was determined by flow cytometry using a FACScan cytofluorimeter and the FACSDIVA software (Becton Dickinson, San Jose, CA).

For lymphocyte analyses, mouse spleens were placed in 3 mL of media (i.e., RPMI 1640 with 10% fetal bovine serum) in a six-well plate. Using sterile forceps, the spleen was placed on a sterile wire mesh screen and pushed through with the plunger of a 10-mL syringe into a 50-mL tube. The cells were pelleted by centrifugation (300-400 × *g*) for 5 min at 4°C, and the supernatant was aspirated. After standard lysis of erythrocytes and washing with PBS, the cell number in the spleen cell suspension was counted. Cells (5×10^5) were double-labeled with anti-CD4 (phycoerythrin)/anti-CD3 (FITC) and anti-CD8 (phycoerythrin)/anti-CD3 (FITC; Becton Dickinson, Franklin Lakes, NJ) and processed on FACSDiva (Becton Dickinson, Franklin Lakes, NJ).

For apoptosis analysis, SCCVII and O12 tumor cells were incubated for 24 h at which time 250 μmol/L lactoferrin was added to the media. The assay was done at 10 min, 20 min, 1 h, and 4 h after exposure to the lactoferrin. The cells were washed by resuspending in 500 μL cold (2°C to 8°C) 1× PBS, pelleted by centrifugation, and resuspended in Annexin V incubation reagent (which contains propidium iodide) at a concentration of 1×10^5 to 1×10^6 cells per 100 μL. Cells were incubated in the dark for 15 min before being collected by centrifugation. Cells were resuspended in 100 μL 1× binding buffer containing fluorescent streptavidin conjugate and incubated in the dark for 15 min at 18°C to 24°C. After calibration of the flow cytometer, samples will be analyzed within 1 h for maximal signal. Treated cells were also stained separately with Annexin V and propidium iodide to define the boundaries of each population.

Quantitative real-time reverse transcription-PCR. Cells were plated into 100-mm dishes at 5×10^6 per dish. After incubation at 37°C for 24 h, the cells were exposed to lactoferrin at 250 μmol/L. After another 24 h, the cells were harvested. Total RNA was extracted from 1×10^7 cells using Qiagen's RNeasy Mini kit (Qiagen, Valencia, CA) according to the manufacturer's directions. The RNA quality was exclusively evaluated by denaturing agarose gel electrophoresis. Cell cycle microarrays were done according to the manufacturer's instructions (Superarray, Frederick, MD). To verify the microarray data, real-time quantitative reverse transcription-PCR was done with a LightCycler 2.0 Instrument, LightCycler FastStart DNA Master^{plus} SYBR Green I kit, and LightCycler DNA control kit (Roche, Indianapolis, IN) according to the manufacturer's protocol. The following LightCycler conditions were used: precycling hold at 95°C for 10 min followed by 45 cycles of denaturation at 95°C for 10 s, annealing at 60°C for 10 s, and extension at 72°C for 12 s. The fluorescence was measured at the end of each cycle to construct amplification curves. To confirm amplification specificity, the PCR products were subjected to a melting curve analysis. Quantitation of transcripts was calculated based on a titrated standard curve co-run in the same experiment and calibrated with the expression level of a housekeeping gene (*β-actin*). All samples were done in triplicate. The primer sequences are shown in Table 1.

Luminex assay for cellular cytokines. SCCVII cells (1×10^5) were incubated in 25-cm^2 flasks overnight. The following morning, the medium was changed, and 200 μmol/L lactoferrin was added. After 24 h, the medium was removed and centrifuged, and the supernatant was collected for Luminex analysis per manufacturer's instructions (Luminex, Austin, TX).

The plates were read using Luminex technology and IS software, and the final concentrations are calculated using Upstate multiplexing software (Upstate, San Francisco, CA). Statistical analysis was done using Student's *t* test.

In vivo *CD3 depletion.* Four- to 6-week-old C3H/HeJ females were injected with 200 μg of purified anti-CD3 (145-2C11) monoclonal antibody (hamster IgG, anti-murine CD3, produced in our lab) on days −1, 0, and 7 by i.p. The mice were divided into two groups (non–lactoferrin-treated control and lactoferrin-treated mice) with five mice in each group. SCCVII cells (1×10^5) were injected into the flanks of each mouse with hypodermic method on day 0. On day 5, the designed treatment was then done. For the lactoferrin-treated groups, lactoferrin was delivered by gavage feeding at doses of 65 mg/kg/d from days 5 to 14. Control mice were treated with PBS. No anesthesia was used for oral gavage feeding. The tumor growth was evaluated every other day from day 5, and the tumors were measured in two dimensions with calipers. The tumor volume was calculated by formula (width^2 × length) / 2. The mice were sacrificed on day 15. The tumors were harvested and were embedded in ornithine carbamyl transferase for immunohistochemistry studies. Blood and spleen were collected for flow cytometry analysis.

Immunohistochemistry. Tumors were harvested on day 15 and then immediately embedded in ornithine carbamyl transferase. Five-micrometer-thick cryostat sections were cut, mounted on Superfrost plus slides (Fisher, Pittsburgh, PA), and then fixed in ice-cold acetone for 5 min. After the slides were air-dried for 30 min, standard staining

Table 1. Reverse transcription-PCR primer sequences

Gene	Primer, forward (5′→3′)	Primer, reverse (5′→3′)	Size	Genbank accession no.
Cyclin D1	GAACAAACAGATCATCCGCAAAC	GCGGTAGTAGGACAGGAAGTTG	166	NM_053056
P^{19}	AGTCCAGTCCATGACGCAG	CATCAGGCACGTTGACATCAG	88	NM_079421
β-Actin	CATGTACGTTGCTATCCAGGC	CTCCTTAATGTCACGCACGAT	250	NM_001101

procedure was done for the presence of infiltration of CD4 and CD8. The slides were rinsed with PBS to remove the ornithine carbamyl transferase. After that, the endogenous peroxidase activity was blocked by incubating the slides in 0.3% H_2O_2 solution in PBS for 10 min. The slides were rinsed in PBS and incubated with 3% fetal bovine serum in PBS for 30 min at room temperature to block the nonspecific binding. The sections were then incubated for 1 h with monoclonal antibodies (purified rat anti-mouse CD4 and purified rat anti-mouse CD8; BD PharMingen, Indianapolis, IN). After washing with PBS, the sections were incubated for 30 min with biotinylated anti-rat IgG (H+L) secondary antibody (Vector Laboratories, Burlingame, CA). The slides were washed with PBS again and incubated for 30 min with ABC reagent (Vector Laboratories). After washing with PBS once more, the slides were incubated in the 3,3′-diaminobenzidine (BD PharMingen) substrate solution for about 10 min. The slides were finally washed in water and counterstained with hematoxylin (Vector Laboratories) to facilitate routine light microscopic. Spleen sections served as positive control. Each section was counted thrice, and the mean was calculated. Statistical analysis was done using Student's *t* test.

Gastrointestinal coculture. Four- to 6-week-old C3H/HeJ female mice were euthanized, and the intestine was harvested from stomach to cecum. Fat and surrounding tissues were removed, and the intestine was irrigated and flushed with wash buffer containing HBSS supplemented with fetal bovine serum, glutamine, penicillin, gentamicin, streptomycin, and amphoteracin B. The tissue was longitudinally incised, rewashed, and transferred to 100 × 15 mm dish with 15 mL of complete DMEM with/without 250 μmol/L lactoferrin and cultured at 37°C with 5% CO_2 for 1, 4, and 8 h. Supernatants were collected at each time point, centrifuged, and analyzed by IL-18 ELISA (R&D Systems. Minneapolis, MN).

Results

***Lactoferrin inhibits growth of human and murine SCC cell lines* in vitro.** Although others have shown that lactoferrin inhibits tumor cell growth *in vitro*, we sought to evaluate the effect of lactoferrin on the growth of both murine and human SCC cell lines. Recombinant human lactoferrin induces a dose-dependent growth inhibition of cancer cell growth via MTT assay (Fig. 1). This was consistent in all cell lines tested. To show that this growth was not dependent on the iron-binding ability of lactoferrin, lactoferrin was saturated with iron at 2:1 molar ration (iron/lactoferrin) for 10 min before adding it to the medium. The growth inhibition was unaffected by iron saturation. These results show that lactoferrin inhibits cancer cell growth via an iron-independent but dose-dependent mechanism.

Lactoferrin induces NF-κB activation in SCC cell lines. Based upon the previously published data that lactoferrin inhibits NF-κB activity, we hypothesized that lactoferrin would decrease constitutive activation of cellular NF-κB. UMSCC9, SCCVII, and UMSCC11B cell lines were incubated with lactoferrin (250 μmol/L), and nuclear extracts were harvested at specific time points. There was increased NF-κB activity at 4 h of lactoferrin exposure that returned to baseline by 24 h (Fig. 2A). The experiment was then repeated using electrophoretic mobility shift assay, which confirmed the induction of active NF-κB (Fig. 2B). Cells were then incubated for 4 h in medium with lactoferrin (250 μmol/L) and in the presence and absence of IL-1α as a positive control. Cell extracts were collected, and the NF-κB ELISA confirmed induction of NF-κB equal to that of the IL-1α. When lactoferrin and IL-1 were combined in the medium, the induction was greater than IL-1 alone for the initial 16 h (P = 0.02, 1 h; P = 0.004, 4 h; P = 0.05, 8 h; P = 0.01, 16 h) and equal to the IL-1 at 24 h (P = 0.8). These results were confirmed with electrophoretic mobility shift assay shown in Fig. 2B and repeated with SCCVII cell lines (data not shown). These results do not support our initial hypothesis and show that lactoferrin up-regulates NF-κB activity. Based upon these experiments, NF-κB likely does not contribute to lactoferrin-induced growth inhibition.

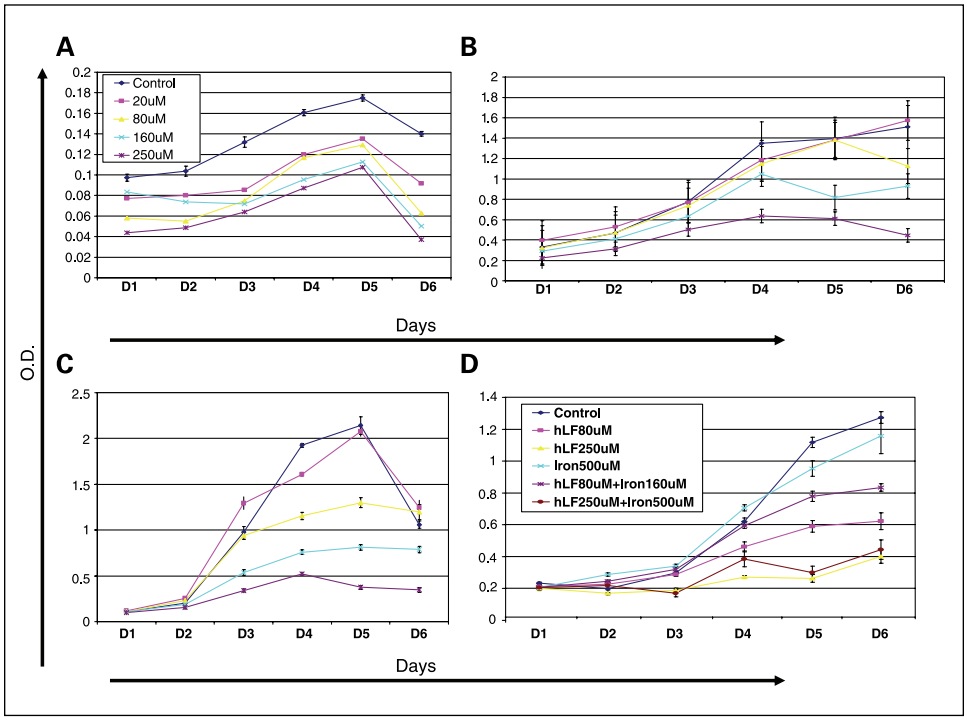

Fig. 1. Murine and human SCC cell lines were cultured in medium containing increasing doses of lactoferrin in doses ranging from 0 to 250 μmol/L. Daily MTT assays were done to assess cell growth. *A,* human cell line UMSCC9 cultured with varying doses of lactoferrin in the medium. There is a dose-dependent decrease in cell number from day 3 and beyond (P < 0.05). *B,* murine cell lines O12 cultured with varying doses of lactoferrin in the medium. There is a dose-dependent decrease in cell number from day 3 and beyond (P < 0.05). *C,* human cell line SCCVII cultured with varying doses of lactoferrin in the medium. *D,* O12 cells were cultured with varying doses of lactoferrin as well as molar ratios of iron to saturate the lactoferrin. The iron-binding state of lactoferrin had no effect on tumor. OD, absorbance.

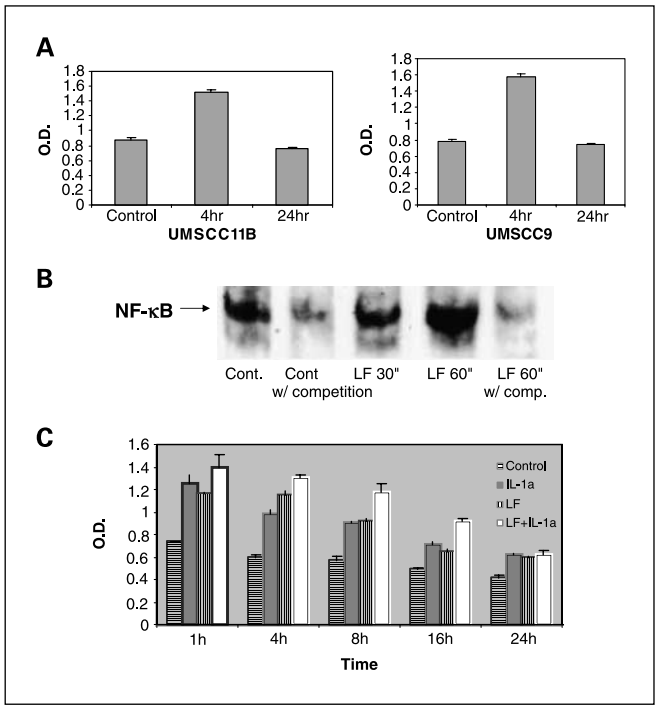

Fig. 2. Lactoferrin induces NF-κB activation in HNSCCA. *A,* UMSCC9 and UMSCC11B cell lines were cultured with lactoferrin (250 μmol/L) for 4 and 24 h. Nuclear extracts were harvested, and ELISA for the p50 subunit was done and read on a plate reader at 450 nm. Within 4 h, lactoferrin induced activation and nuclear translocation of NF-κb compared with controls ($P = 0.04$). At 24 h of lactoferrin exposure, the amount of activated NF-κB returns to that of control tumors ($P = 0.27$). *B,* to confirm the NF-κB activation, UMSCC9 cells were cultured with lactoferrin (*LF*; 250 μmol/L), and nuclear extracts were harvested at 30 and 60 min. Electrophoretic mobility shift assay was done for activated subunit of NF-κB and read on photopaper. There is specific increase in NF-κB binding at both 30 and 60 min, which can be alleviated with unlabeled competitive sequence. *C,* UMSCC9 cell lines were cultured with lactoferrin (250 μmol/L), IL-1α (500 pg/mL as positive control), and lactoferrin + IL-1α. Nuclear extracts were harvested, and an ELISA for the p50 subunit was done and read on a plate reader at 450 nm. At all time points, there was increased activated NF-κB compared with controls ($P < 0.05$). When compared with IL-1α alone, the amount of activated NF-κB in the lactoferrin + IL-1α group was greater at 1 h ($P = 0.017$), 4 h ($P = 0.003$), and 16 h ($P = 0.013$).

Lactoferrin inhibits cell cycle progression with arrest at the G_1-G_0 checkpoint. It has previously been reported that lactoferrin induces G_1-G_0 growth arrest in head and neck and breast cancer cell lines. To determine the mechanism of growth inhibition in our cell lines, both SCCVII and O12 cell lines were plated and cultured overnight. After 24 h, the medium was changed, and 250 μmol/L lactoferrin was added to the media. The cells were cultured for 24 and 48 h and were harvested and analyzed by flow cytometry. In both cell lines and at both time points, there were increases in cells in the G_1-G_0 phase compared with controls, with resultant decreases in the percentage of cells in the S phase (Table 2). We did cell cycle microarrays (Superarray), which showed decreases in cyclin D1 in lactoferrin-treated controls, with resultant increases in p19 (data not shown). This was confirmed via quantitative PCR (Fig. 3A). To determine whether lactoferrin induces apoptosis, cells were cultured in 250 μmol/L lactoferrin. At six time points ranging from 2 to 48 h, they were costained with Annexin V and propidium iodide and were analyzed with flow cytometry. Tumor necrosis factor-α was used as a positive control. There was no induction of apoptosis at any time point in the lactoferrin group (data not shown). These results show that lactoferrin does not induce apoptosis in HNSCCA and inhibits growth via cell cycle arrest.

Lactoferrin changes the production of proinflammatory cytokines in SCC. We have previously published that SCC of the head and neck produce proinflammatory cytokines. To determine whether lactoferrin would alter this production, the supernatant of SCCVII cultured in lactoferrin was collected, and a Luminex assay was done. Significant decreases in granulocyte macrophage colony-stimulating factor ($P = 0.01$), IL-6 ($P = 0.04$), tumor necrosis factor-α ($P = 0.05$), and IL-8 were observed (Table 3). Marked increases in IL-10 were noted and, as expected, no detectable changes in IL-18. These results show that lactoferrin can induce changes in the inflammatory milieu of tumor cells and specifically can inhibit the production of proinflammatory and prometastatic cytokines.

Oral lactoferrin inhibits the growth of murine SCC and induces lymphocytic infiltration of tumors. We sought to show that oral lactoferrin would induce tumor inhibition in the mouse model. It has been previously shown that oral lactoferrin can increase circulating and splenic numbers of $CD4^+$ and $CD8^+$ cells, but it has never been shown that this results in increased infiltration of tumors by these cells. We designed an experiment in which C3H/HeJ mice were anesthetized, and 0.1-mL suspension of 5×10^5 SCCVII cells was implanted on the flank or the floor of mouth. Tumors were allowed to grow for 5 days. Mice were

Table 2. Lactoferrin induces G_1-G_0 growth arrest

Cell line	Treatment	% G_0-G_1	% S	% G_2-M
SCCVII	Control (24 h)	37.38	49.21	13.4
	250 μmol/L lactoferrin (24 h)	57.96	29.36	12.68
012	Control (24 h)	37.18	40.92	21.9
	250 μmol/L lactoferrin (24 h)	46.6	35.46	18.14
SCCVII	Control (48 h)	40.47	46.69	12.84
	250 μmol/L lactoferrin (48 h)	56.55	28.89	14.56
012	Control (48 h)	26.51	45.18	28.31
	250 μmol/L lactoferrin (48 h)	47.43	35.24	17.33

NOTE: SCCVII and O12 cells (1×10^5) were incubated in 25-cm^2 flasks, and lactoferrin (250 μmol/L) was added to the medium. At 24 h, cells were trypsinized, stained, and analyzed using flow cytometry. Lactoferrin induces growth arrest at the G_0-G_1 checkpoint compared with controls.

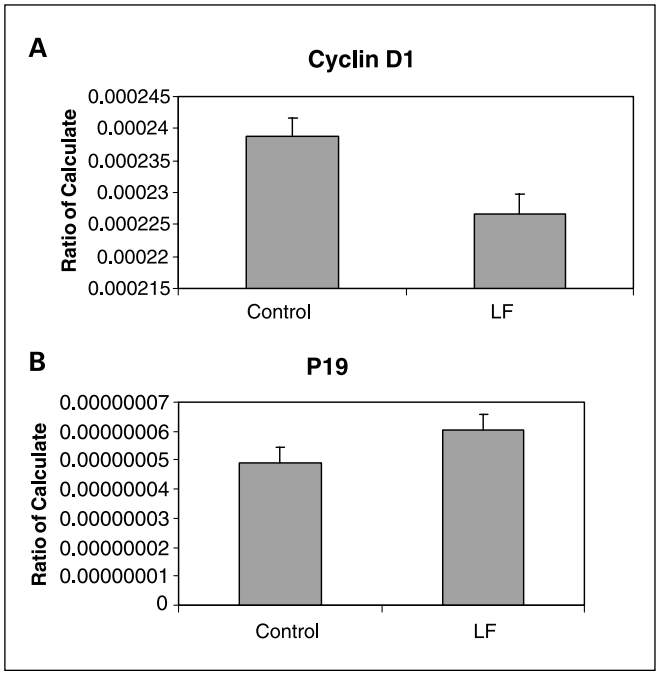

Fig. 3. Lactoferrin induces G_1-G_0 growth arrest. *A,* cells were exposed to lactoferrin (250 μmol/L) for 24 h. RNA was harvested, and real-time quantitative reverse transcription-PCR was done to evaluate for changes in cyclin D1. Lactoferrin exposure induced a decrease in cyclin D1. *B,* cells were exposed to lactoferrin (250 μmol/L) for 24 h. RNA was harvested, and real-time quantitative reverse transcription-PCR was done to evaluate for changes in P19. Lactoferrin exposure induced an increase in P19. These changes in cyclin D1 and P19 are the likely mechanism whereby the G_1-G_0 growth arrest occurs.

then treated with lactoferrin via gastric gavage for 10 days. The mice with orthotopic tumors were sacrificed and had the tumors measured on day 10 of lactoferrin dosing. Mice with flank tumors were measured daily during lactoferrin dosing. The volume of the orthotopic tumors in mice receiving lactoferrin was 62% to 75% reduced compared with controls ($P < 0.002$; Fig. 4A). The volume of flank tumors in lactoferrin-treated mice were reduced by 67% to 70% of that in control mice (Fig. 4B). Mice were also treated with fetal bovine serum to evaluate whether the reduction of tumor volume was due to the presence a foreign protein. There was no difference in tumor volume in mice receiving fetal bovine serum and control mice. Tumors were harvested after 10 days of oral lactoferrin and stained for $CD4^+$ and $CD8^+$ lymphocytes within the tumors. Stained cells were counted per high powered field, and there were marked increases in the numbers of both $CD4^+$ and $CD8^+$ cells infiltrating the tumors compared with non–lactoferrin-treated animals (Fig. 4C and D). These results show that oral lactoferrin dramatically inhibits HNSCCA growth *in vivo* and induces lymphocytic infiltration into the tumors of treated mice.

Tumor growth inhibition in lactoferrin-treated mice is abrogated by depleting mice of lymphocytes. Although we have shown that lactoferrin will increase the lymphocyte population within the tumors, we hypothesized that this was the mechanism of tumor inhibition. To test this hypothesis, we depleted mice of $CD3^+$ cells and repeated the experiment. C3H/HeJ mice were treated with three doses of 200 μg of anti-CD3 monoclonal antibody given i.p. This protocol was tested in control mice to assure depletion in the serum and spleen (data not shown). In tumor-bearing mice, antibody was delivered for 2 days before SCCVII implantation and on day 3 of lactoferrin dosing. Tumors, serum, and spleens were harvested after 10 days of lactoferrin treatment, and flow cytometry for CD3 was done. There was successful depletion to <1% of cells in both spleen (Fig. 5A) and serum (data not shown). Tumor growth curves in CD3-depleted mice revealed no differences in tumor volume in lactoferrin-treated mice compared with controls (Fig. 5B). To confirm this, the tumors were analyzed for $CD3^+$ cells by immunohistochemistry, and there was no difference in tumor staining between the lactoferrin-treated group and controls (Fig. 5C and D).

To confirm that immunomodulation is a mechanism of lactoferrin-induced tumor inhibition, we repeated oral dosing experiments on BALB/c nude mice. In these animals, the lactoferrin-treated animals has significantly larger tumors ($P = 0.01$) after 10 days of lactoferrin (Fig. 6). These data show that immunomodulation is a major mechanism of lactoferrin-induced tumor inhibition, and that the G_1-G_0 growth arrest noted *in vitro* does not seem to significantly contribute to tumor inhibition *in vivo*.

Lactoferrin induces IL-18 production by the intestinal mucosa. To determine whether the increased quantity of i.t. lymphocytes are related to alteration of intestinal cytokine production in the gut by enteral lactoferrin dosing, we did isolated intestinal coculture experiments. The intestines from mice were

Table 3. Lactoferrin inhibits SCC production of proinflammatory cytokines

	Control (pg/mL)	200 μmol/L lactoferrin (pg/mL)	*P*	Medium (pg/mL)
GM-CSF	55.9 ± 10.8	7.78 ± 9.44	0.013	<1.2
IL-6	205.72 ± 69.04	38.40 ± 7.62	0.038	<1.2
IL-10	<1.2	6.52 ± 0	NA	<1.2
KC (IL-8)	>5,000	1,728.88 ± 405.3	NA	<1.2
TNF-α	7.32 ± 0.68	3.385 ± 0.26	0.048	2.85
IL-18	<1.2	<1.2	NA	<1.2

NOTE: SCCVII cells (1×10^5) were incubated in 25-cm^2 flasks. Cells were cultured overnight, at which time the medium was changed, and 250 μmol/L lactoferrin was added. The medium was collected after 24 h, and Luminex assay for cytokines was done. There is a lactoferrin-related decrease in GM-CSF, IL-6, IL-2, KC (IL-8), and TNF-α over controls and medium. There was an increase in IL-10 in the lactoferrin-treated cells, and as expected, no detectable IL-18.
Abbreviations: GM-CSF, granulocyte macrophage colony-stimulating factor; TNF-α, tumor necrosis factor-α; NA, not available.

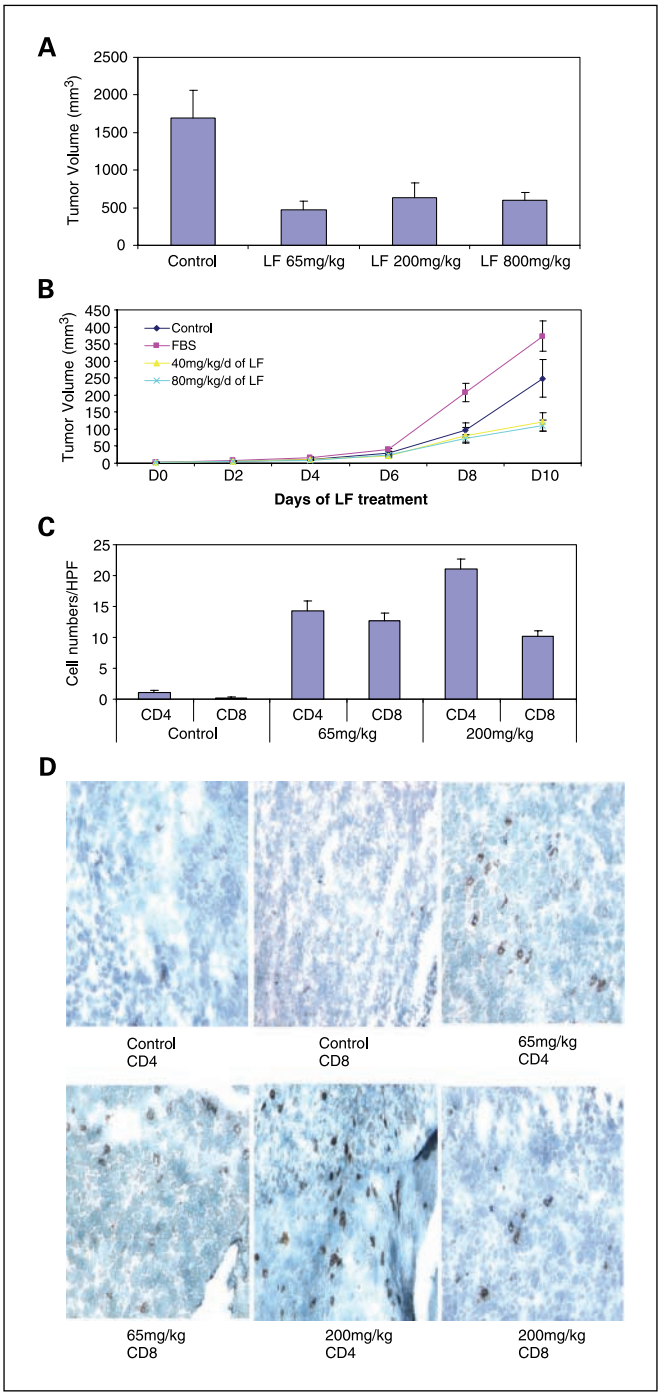

Fig. 4. Oral lactoferrin inhibits the growth of SCCVII tumors in the murine model and induces lymphocytic infiltration into tumors. *A,* 5×10^6 cells of SCCVII were implanted orthotopically in the floor of mouth of mice. The tumors were allowed to grow for 5 d, and the volume was measured. For 10 subsequent days, the mice were given varying doses of lactoferrin via oral gavage. After the last lactoferrin dose, mice were sacrificed, and the tumors were measured and harvested. After 10 d of lactoferrin dosing, the tumor volumes reduced by 62% to 75% compared with control mice. *B,* to assess evaluate the tumor growth curves, the same model was followed, except that SCCVII were injected on the animal flank. Tumor volumes were measured daily during the 10 d of lactoferrin gavage. Fetal bovine serum (*FBS*) was used as a foreign protein control. After 10 d of lactoferrin dosing, the tumor volumes reduced by 67% to 70% compared with serum control mice. *C* and *D,* tumors were harvested, and immunohistochemistry was done for $CD4^+$ and $CD8^+$ cells within the tumor. Tumors were photographed, and positively staining cells were counted per high power field in triplicate. Tumors in lactoferrin-treated mice had significant increases in the number of $CD4^+$ and $CD8^+$ lymphocytes within the tumor ($P < 0.001$).

incised longitudinally and maintained in either complete DMEM or DMEM supplemented with 250 μmol/L lactoferrin. After 1, 4, and 8 h, supernatants were collected, and IL-18 ELISA was done. The quantity of IL-18 in the lactoferrin-exposed mucosa was four times greater than control mucosa (Fig. 7). There was no difference in concentration of IL-8 (KC) or IL-6 in the supernatant when compared with controls (data not shown).

To determine whether increased intestinal production of IL-18 correlated with serum IL-18, serum IL-18 was measured in tumor-bearing C3H/HeJ mice receiving 10 days of oral lactoferrin. There was no significant difference ($P = 0.06$) in measurable serum IL-18 between lactoferrin-treated and control mice (Fig. 7).

These data show that lactoferrin up-regulates localized intestinal production of the IL-18, a potent $CD4^+$ chemoattractant, but does not significantly change serum IL-18 concentration.

Discussion

Lactoferrin inhibits the growth of HNSCCA. Despite our *in vitro* studies showing direct growth inhibition via G_1-G_0 blockade, NF-κB activation, and reduction of cellular proinflammatory cytokines, the mechanism of tumor control *in vivo* seems to be regulated primarily by the cellular arm of the immune response. Because of the favorable toxicity profile and availability of this drug, our data support the study of lactoferrin for the treatment of HNSCCA.

Because lactoferrin-induced growth inhibition has been previously attributed to intrinsic and immunologic control of cellular proliferation, we sought to define the relative input of each by using *in vitro* and *in vivo* studies. In this current study, we have shown that human recombinant lactoferrin inhibits both human and murine SCC line proliferation in a dose-dependent manner. This growth inhibition is independent of the iron-binding state and is not due to NF-κB down-regulation. We have previously shown that inhibition of NF-κB activation in SCC cell lines decreases cell viability (15, 36), and thus expected, this would be a mechanism of lactoferrin. We had hypothesized that growth inhibition may be due directly to down-regulation of NF-κB, which is constitutively activated in the cell lines used in this study, but our present results show that lactoferrin causes an initial increase in active NF-κB binding followed by return to pretreatment levels (37). The increase in active NF-kb is transient and may explain why we were unable to detect increases in NF-κB–dependent cytokines at 24 h posttreatment.

These findings are in contrast to other published works that showed that lactoferrin inhibits NK-κB activation in monocytes and rat colon cells (13, 38). Our data, as well as that of Oh, confirm that lactoferrin up-regulates NF-κB in cancer cell lines (39). It is possible that the effects of lactoferrin on NF-κB activity may differ based upon the cell type (monocytes versus carcinoma cell lines), and it seems from our results that the lactoferrin effect on NF-κB is not directly causative of growth inhibition.

Lactoferrin alters the cytokine milieu of cancer cells lines. This is important in the context that HNSCCA lines produce proinflammatory cytokines that allow tumor propagation

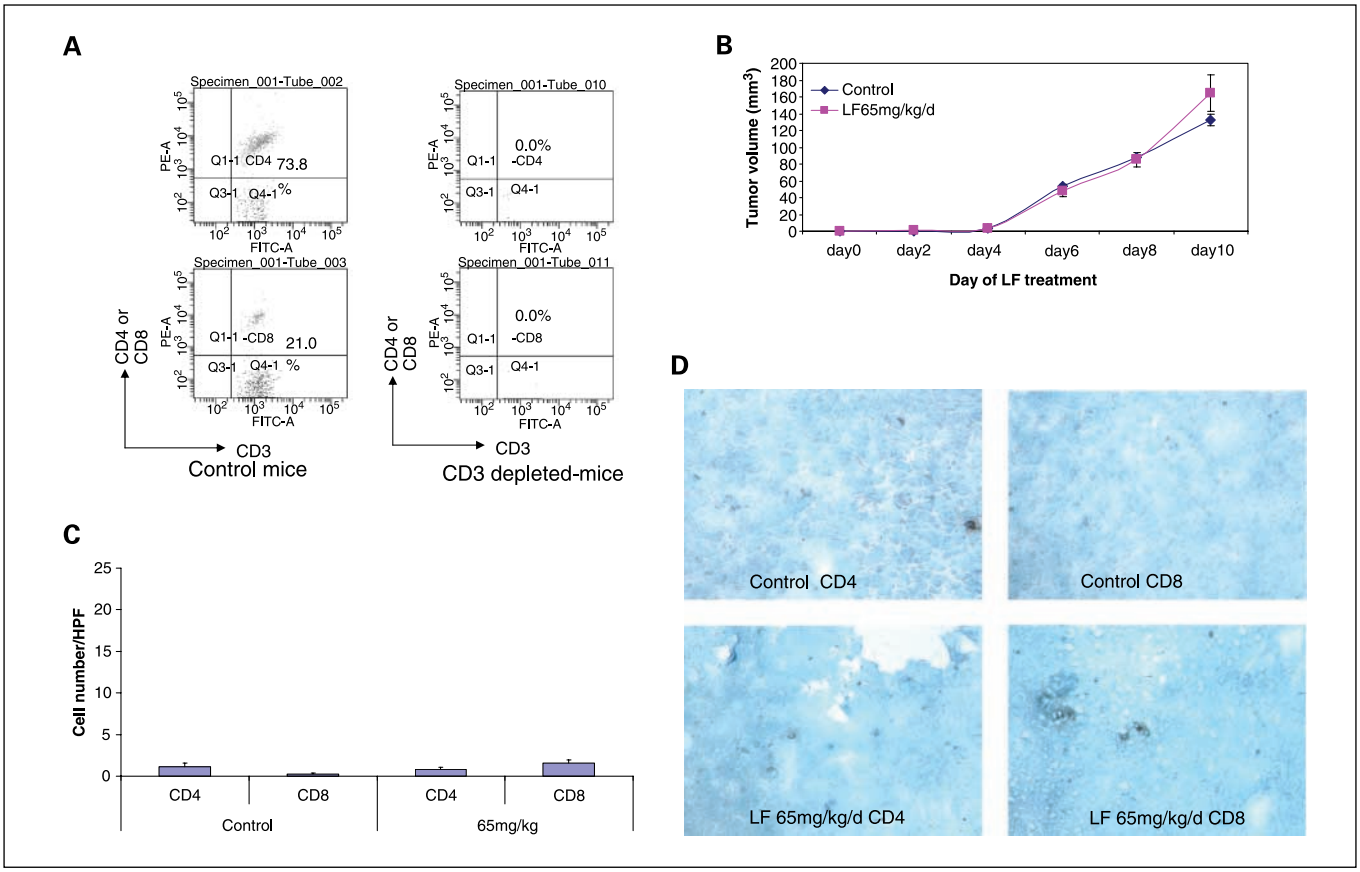

Fig. 5. Lactoferrin-induced tumor growth inhibition is abrogated by depleting tumors of CD3. Mice were depleted of $CD3^+$ cells using 200 mg of i.p. anti-CD3 on days −1, 0, and 7 after SCCVII injection. Lactoferrin was given via oral gavage for 10 d starting at day 5 after tumor implantation, and tumors were measured daily. Tumors and spleens were harvested after the last lactoferrin dose. *A,* spleens were stained for $CD3^+$, $CD4^+$, and $CD8^+$ cells and analyzed by flow cytometry. There was complete depletion of splenic $CD3^+$ cells compared with control mice. *B,* tumor volumes were measured during the 10 days of lactoferrin dosing. In these $CD3^+$ depleted mice, there was no significant difference in tumor volume between mice receiving lactoferrin and controls. *C* and *D,* tumors were harvested, and immunohistochemistry was done for $CD4^+$ and $CD8^+$ cells within the tumor. Tumors were photographed, and positively staining cells were counted per high power field in triplicate. Tumors in lactoferrin-treated mice had no difference in the numbers of $CD4^+$ and $CD8^+$ lymphocytes within the tumor.

in vitro and are thought to contribute to the malignant phenotype of head and neck cancer (15–17, 40). We have found shown that lactoferrin decreases the cellular production of granulocyte macrophage colony-stimulating factor, IL-6, KC (IL-8), and tumor necrosis factor-α and increases the production of IL-10. Clinically, IL-6, IL-8, granulocyte macrophage colony-stimulating factor, and IL-1–inducible acute phase proteins are all present in significantly higher levels in the serum of head and neck cancer patients than in age-matched controls (17). IL-8 promotes angiogenesis and tumor metastasis in the lung SCC and granulocyte macrophage colony-stimulating factor promotes metastasis of head and neck SCC (41, 42). We had hypothesized that down-regulation of these cytokines may have contributed to lactoferrin inhibiting the growth of these tumors. It was these *in vitro* immunomodulatory functions of lactoferrin that enticed us to look at this potential mechanism *in vivo*.

Once we identified that lactoferrin induced direct cellular growth inhibition, we aimed to determine the mechanism by which this occurred. In all cell lines tested, we found G_1-G_0 arrest compared with controls. Using microarray and quantitative PCR, we specifically identified decreases in cyclin D1 and increases in p19 as the likely mechanism for this cell cycle arrest. These data correspond with others that have shown that lactoferrin-induced growth arrest was caused by cell cycle inhibition at the G_0-G_1 checkpoint (11, 12). Xiao reported that this was associated with an increase in p27 protein,

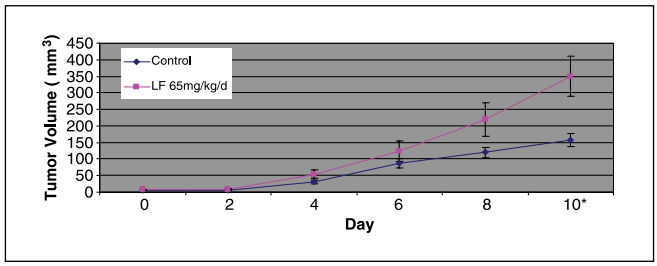

Fig. 6. Lactoferrin does not inhibit tumor growth in athymic mice. Cells of SCCVII (5×10^6) were implanted into the flank of BALB/c nude mice. The tumors were allowed to grow for 5 d, and the volume was measured. For 10 subsequent days, the mice were given varying doses of lactoferrin via oral gavage. After the last lactoferrin dose, mice were sacrificed, and the tumors were measured and harvested. In this athymic model, there were no differences between lactoferrin-treated mice and control mice until the 10th day of lactoferrin, when the lactoferrin-treated mice had larger tumors than control mice. *, $P = 0.01$, statistical significance.

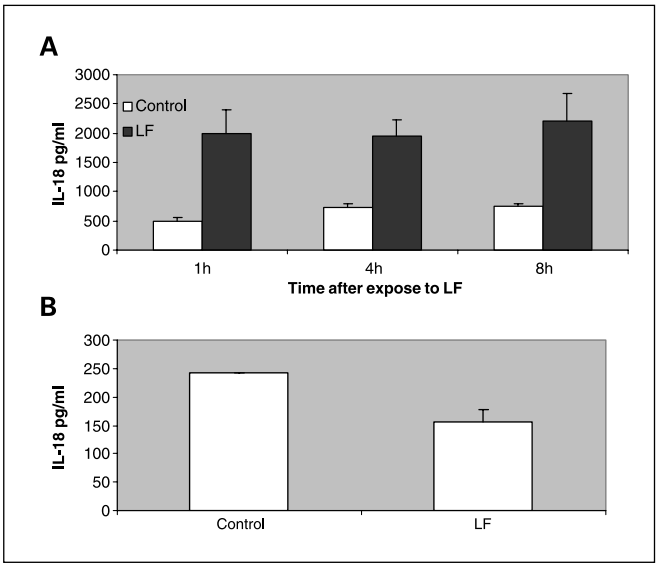

Fig. 7. Lactoferrin increases intestinal production of IL-18. *A,* the intestinal mucosa from C3H/HeJ mice was isolated and cocultured with 250 μmol/L lactoferrin. Supernatant was collected and measured for IL-18 concentration using ELISA. There was 400% increase in IL-18 in the lactoferrin group compared with control medium ($P = 0.01$). *B,* 5×10^6 cells of SCCVII were implanted orthotopically in the floor of mouth of mice. The tumors were allowed to grow for 5 d. For 10 subsequent days, the mice were given 65 mg/kg dose of lactoferrin via oral gavage. After the last lactoferrin dose, serum was collected and measured for IL-18. There was no significant difference in serum IL-18 between treated and control mice ($P = 0.06$).

accompanied by decreased phosphorylation of retinoblastoma protein, and suppression of cyclin E; however, these were unchanged in our cell lines (11). Using our cell line data, we focused on discerning the relative contribution of this growth inhibition *in vivo*.

Oral delivery of lactoferrin results in decreased tumor growth. Specifically in this study, we showed that oral lactoferrin inhibits tumors while inducing lymphocytic infiltration into tumors. These data are consistent with data that lactoferrin inhibits growth of mouse tumors (25, 26, 43). It has been shown that when given i.v., orally (via gavage), or directly injected into tumors, the greatest inhibition of tumor growth occurs with oral dosing (26). Oral lactoferrin has been shown to stimulate intestinal IL-18 production by 3- to 7-fold, which increases splenic production of natural killer cells and serum $CD8^+$ cells (26). It has been shown to reconstitute the circulating and splenic $CD4^+$ and $CD8^+$ cell population in mice treated with cyclophosphamide (21). Our study has elucidated that aside from this increased serum and splenic lymphocytes, oral lactoferrin induces infiltration of these cells within tumors. What is perhaps the most exciting about these data is that that this occurs in the SCCVII cell line, which is poorly immunogenic and rapidly growing (33, 44, 45).

The effect of oral lactoferrin on *in vivo* tumor growth seems to be largely due to this immunomodulation. Although this has been previously hypothesized, these are the first data to support this hypothesis. We found that by depleting mature lymphocytes with an anti-$CD3^+$ antibody, the entire antitumor effect is abrogated. We were able to identify no differences in tumor volume or lymphocytic infiltration between control mice and CD3-depleted mice that were treated with lactoferrin. Nude mice (which have intact natural killer cells) actually had slightly increased tumor size in the after 10 days of lactoferrin treatment. This supports our premise that it is lymphocytes and not natural killer cells that contribute to tumor inhibition in lactoferrin-treated animals. The increased tumor size in lactoferrin-treated athymic mice after 10 days of treatment may improve nutrition from gavage with lactoferrin.

We now know from our work that the tumor inhibition obtained from oral lactoferrin dosing is largely, if not solely, due to immunomodulation resulting in lymphocytic infiltration in tumors. The mere up-regulation of the quantity of T lymphocytes does not completely explain the mechanism of lactoferrin; there is a marked increase of lymphocytes within the tumors in the lactoferrin-treated group. Although lactoferrin up-regulates gut production of IL-18, a $CD4^+$ cell chemoattractant, IL-18 is not produced the tumors or by cell lines exposed to lactoferrin, and lactoferrin is not able to measured in the serum in orally treated animals (26, 46). This brings in to question the mechanism by which the lymphocytes are becoming sensitized to tumor-specific antigens. The mechanism by which the immunomodulation occurs will be better elucidated by performing experiments on IL-18 knockout mice and dendritic cell knockout mice and analysis of the tumor-infiltrating lymphocytes.

To further understand the potential of lactoferrin as a chemotherapeutic agent, one must examine its safety profile. In published studies, there have been no signs of toxicity in mice or monkeys treated with oral and i.v. lactoferrin up to 5,000 mg/kg. In human studies, no toxicity in i.v. lactoferrin have been reported (47). In a recent non–small cell lung cancer trial, 10 patients were given oral lactoferrin up to 9 g/d without any hematologic, hepatic, or renal toxicities (48). This exceptional safety profile makes lactoferrin attractive as a primary chemotherapeutic agent in addition to being a possible adjuvant.

At the oral doses delivered, we were unable to show a dose-response relationship for oral lactoferrin despite a large dosing range from 40 to 800 mg/kg. We hypothesize that there is a low quantity of lactoferrin receptors in the gut that are entirely saturated with even the lowest dose tested. Teleologically, this is likely due to the moderate concentration of lactoferrin in human breast milk (970 mg/dL); thus, there would be little purpose for high concentration of receptors in the gut (49). The small intestine lactoferrin receptor is rapidly saturated by lactoferrin, which has a small dissociation constant with its receptor (29, 50). Further studies with significantly smaller concentrations of lactoferrin may need to be done to show a dose-response relationship or saturation kinetics. With the known concentration of lactoferrin in human breast milk, the anticancer properties that we have shown may be clinically related to the lower rate of malignancies in breast-fed infants (8–10).

These data provide insight into the antitumor effect of human recombinant lactoferrin on SCC of the head and neck and provide a potential strategy for new treatments of head and neck cancer. Lactoferrin can potentially be used as a direct agent via i.t. injection as well as a systemic agent via oral delivery. Although more information regarding the mechanism of oral lactoferrin is needed, these early data show that lactoferrin has potential as a safe and effective means to treat cancers of the head and neck.

References

1. Metz-Boutigue MH, Jolles J, Mazurier J, et al. Human lactotransferrin: amino acid sequence and structural comparisons with other transferrins. Eur J Biochem 1984;145:659–76.
2. Kanyshkova TG, Buneva VN, Nevinsky GA. Lactoferrin and its biological functions. Biochemistry (Mosc) 2001;66:1–7.
3. Levay PF, Viljoen M. Lactoferrin: a general review. Haematologica 1995;80:252–67.
4. Masson PL, Heremans JF, Schonne E. Lactoferrin, an iron-binding protein in neutrophilic leukocytes. J Exp Med 1969;130:643–58.
5. Ward PP, Uribe-Luna S, Conneely OM. Lactoferrin and host defense. Biochem Cell Biol 2002;80:95–102.
6. Ward PP, Paz E, Conneely OM. Multifunctional roles of lactoferrin: a critical overview. Cell Mol Life Sci 2005;62:2540–8.
7. Cumberbatch M, Dearman RJ, Uribe-Luna S, et al. Regulation of epidermal Langerhans cell migration by lactoferrin. Immunology 2000;100:21–8.
8. Breastfeeding and childhood cancer. Br J Cancer 2001;85:1685–94.
9. Mathur GP, Gupta N, Mathur S, et al. Breastfeeding and childhood cancer. Indian Pediatr 1993;30:651–7.
10. Hardell L, Dreifaldt AC. Breast-feeding duration and the risk of malignant diseases in childhood in Sweden. Eur J Clin Nutr 2001;55:179–85.
11. Xiao Y, Monitto CL, Minhas KM, Sidransky D. Lactoferrin down-regulates G_1 cyclin-dependent kinases during growth arrest of head and neck cancer cells. Clin Cancer Res 2004;10:8683–6.
12. Damiens E, El Yazidi I, Mazurier J, Duthille I, Spik G, Boilly-Marer Y. Lactoferrin inhibits G_1 cyclin-dependent kinases during growth arrest of human breast carcinoma. J Cell Biochem 1999;74:486–98.
13. Togawa J, Nagase H, Tanaka K, et al. Lactoferrin reduces colitis in rats via modulation of the immune system and correction of cytokine imbalance. Am J Physiol Gastrointest Liver Physiol 2002;283:G187–95.
14. Zucali JR, Broxmeyer HE, Levy D, Morse C. Lactoferrin decreases monocyte-induced fibroblast production of myeloid colony-stimulating activity by suppressing monocyte release of interleukin-1. Blood 1989;74:1531–6.
15. Wolf JS, Chen Z, Dong G, et al. IL (Interleukin)-1a promotes nuclear factor-kB and AP-1-induced IL-8 expression, cell survival, and proliferation in head and neck squamous cell carcinomas. Clin Cancer Res 2001;7:1812–20.
16. Ondrey FG, Sunwoo JB, Dong G, Chen Z, Bancroft CC, Van Waes C. Constitutive expression of proinflammatory cytokines and survival in head and neck squamous cell carcinoma cell lines. Mol Carcinog 1999;26:119–29.
17. Chen Z, Malhotra PS, Thomas GR, et al. Expression of proinflammatory and proangiogenic cytokines in human head and neck cancer. Clin Cancer Res 1999;5:1369–79.
18. Guillen C, McInnes IB, Baughan DM, et al. Enhanced Th1 response to *Staphylococcus aureus* infection in human lactoferrin-transgenic mice. J Immunol 2002;168:3950–7.
19. Kuhara T, Iigo M, Itoh T, et al. Orally administered lactoferrin exerts an antimetastatic effect and enhances production of IL-18 in the intestinal epithelium. Nutr Cancer 2000;38:192–9.
20. Wang WP, Iigo M, Sato J, Sekine K, Adachi I, Tsuda H. Activation of intestinal mucosal immunity in tumor-bearing mice by lactoferrin. Jpn J Cancer Res 2000;91:1022–7.
21. Artym J, Zimecki M, Kruzel ML. Reconstitution of the cellular immune response by lactoferrin in cyclophosphamide-treated mice is correlated with renewal of T cell compartment. Immunobiology 2003;207:197–205.
22. Bezault J, Bhimani R, Wiprovnick J, Furmanski P. Human lactoferrin inhibits growth of solid tumors and development of experimental metastases in mice. Cancer Res 1994;54:2310–2.
23. Masuda C, Wanibuchi H, Sekine K, et al. Chemopreventive effects of bovine lactoferrin on *N*-butyl-*N*-(4-hydroxybutyl)nitrosamine-induced rat bladder carcinogenesis. Jpn J Cancer Res 2000;91:582–8.
24. Sekine K, Watanabe E, Nakamura J, et al. Inhibition of azoxymethane-initiated colon tumor by bovine lactoferrin administration in F344 rats. Jpn J Cancer Res 1997;88:523–6.
25. Wolf JS, Li D, Taylor RJ, O'Malley BW, Jr. Lactoferrin inhibits growth of malignant tumors of the head and neck. ORL J Otorhinolaryngol Relat Spec 2003;65:245–9.
26. Varadhachary A, Wolf JS, Petrak K, et al. Oral lactoferrin inhibits growth of established tumors and potentiates conventional chemotherapy. Int J Cancer 2004;111:398–403.
27. Shau H, Kim A, Golub SH. Modulation of natural killer and lymphokine-activated killer cell cytotoxicity by lactoferrin. J Leukoc Biol 1992;51:343–49.
28. Suzuki YA, Lonnerdal B. Characterization of mammalian receptors for lactoferrin. Biochem Cell Biol 2002;80:75–80.
29. Suzuki YA, Shin K, Lonnerdal B. Molecular cloning and functional expression of a human intestinal lactoferrin receptor. Biochemistry 2001;40:15771–9.
30. Talukder MJ, Takeuchi T, Harada E. Characteristics of lactoferrin receptor in bovine intestine: higher binding activity to the epithelium overlying Peyer's patches. J Vet Med A Physiol Pathol Clin Med 2003;50:123–31.
31. Hu WL, Mazurier J, Montreuil J, Spik G. Isolation and partial characterization of a lactotransferrin receptor from mouse intestinal brush border. Biochemistry 1990;29:535–41.
32. Hu WL, Mazurier J, Sawatzki G, Montreuil J, Spik G. Lactotransferrin receptor of mouse small-intestinal brush border. Binding characteristics of membrane-bound and triton X-100-solubilized forms. Biochem J 1988;249:435–41.
33. O'Malley BW, Jr., Cope KA, Johnson CS, Schwartz MR. A new immunocompetent murine model for oral cancer. Arch Otolaryngol Head Neck Surg 1997;123:20–4.
34. Beg AA, Finco TS, Nantermet PV, Baldwin AS, Jr. Tumor necrosis factor and interleukin-1 lead to phosphorylation and loss of I kappa B alpha: a mechanism for NF-kappa B activation. Mol Cell Biol 1993;13:3301–10.
35. Renard P, Ernest I, Houbion A, et al. Development of a sensitive multi-well colorimetric assay for active NFkappaB. Nucleic Acids Res 2001;29:E21.
36. Sunwoo JB, Chen Z, Dong G, et al. Novel proteasome inhibitor PS-341 inhibits activation of nuclear factor-kappa B, cell survival, tumor growth, and angiogenesis in squamous cell carcinoma. Clin cancer Res 2001;7:1419–28.
37. Ondrey FG, Dong G, Sunwoo J, et al. Constitutive activation of transcription factors NF-(kappa)B, AP-1, and NF-IL6 in human head and neck squamous cell carcinoma cell lines that express pro-inflammatory and pro-angiogenic cytokines. Mol Carcinog 1999;26:119–29.
38. Haversen L, Ohlsson BG, Hahn-Zoric M, Hanson LA, Mattsby-Baltzer I. Lactoferrin down-regulates the LPS-induced cytokine production in monocytic cells via NF-kappa B. Cell Immunol 2002;220:83–95.
39. Oh SM, Pyo CW, Kim Y, Choi SY. Neutrophil lactoferrin upregulates the human p53 gene through induction of NF-kappaB activation cascade. Oncogene 2004;23:8282–91.
40. Chen Z, Colon I, Ortiz N, et al. Effects of IL-1a, IL-1RA, and neutralizing antibody on proinflammatory cytokine expression by human squamous cell carcinoma lines. Cancer Res 1998;58:3668–76.
41. Smith DR, Polverini PJ, Kunkel SL, et al. Inhibition of interleukin 8 attenuates angiogenesis in bronchogenic carcinoma. J Exp Med 1994;179:1409–15.
42. Young MR, Wright MA, Lozano Y, et al. Increased recurrence and metastasis in patients whose primary head and neck squamous cell carcinomas secreted granulocyte-macrophage colony stimulating factor and contained $CD34^+$ natural suppressor cells. Int J Cancer 1997;74:69–74.
43. Tanaka T, Kawabata K, Kohno H, et al. Chemopreventive effect on bovine lactoferrin on 4-nitroquinoline 1-oxide-induced tongue carcinogenesis in male F344 rats. Jpn J Cancer Res 2000;91:25–33.
44. Strome SE, Voss S, Wilcox R, et al. Strategies for antigen loading of dendritic cells to enhance the antitumor immune response. Cancer Res 2002;62:1884–9.
45. Strome SE, Dong H, Tamura H, et al. B7–1 blockade augments adoptive T-cell immunotherapy for squamous cell carcinoma. Cancer Res 2003;63:6501–5.
46. Komai-Koma M, Gracie JA, Wei XQ, et al. Chemoattraction of human T cells by IL-18. J Immunol 2003;170:1084–90.
47. Ziere B, Van Veen H, Koopman J, Van Berkel P, Nuijens J. Safety, tolerability, and pharmacokinetics of IV. administered rhLF in humans. In: 5th International Conference on Lactoferrin 2001. Alberta (Canada): Pharming Technologies; 2001.
48. Hayes TG, Falchook GF, Varadhachary GR, et al. Phase I trial of oral talactoferrin alfa in refractory solid tumors. Invest New Drugs 2006;24:233–40.
49. Ronayne de Ferrer PA, Baroni A, Sambucetti ME, Lopez NE, Ceriani Cernadas JM. Lactoferrin levels in term and preterm milk. J Am Coll Nutr 2000;19:370–3.
50. Kawakami H, Lonnerdal B. Isolation and function of a receptor for human lactoferrin in human fetal intestinal brush-border membranes. Am J Physiol 1991;261:G841–6.